Characteristics of amnestic patients with hypometabolism patterns suggestive of Lewy body pathology

Jesús Silva-Rodríguez,[1] Miguel A. Labrador-Espinosa,[1,2] Alexis Moscoso,[3] Michael Schöll,[3,4] Pablo Mir[1,2,5] and Michel J. Grothe[1,2,3], for the Alzheimer's Disease Neuroimaging Initiative

A clinical diagnosis of Alzheimer's disease dementia (ADD) encompasses considerable pathological and clinical heterogeneity. While Alzheimer's disease patients typically show a characteristic temporo-parietal pattern of glucose hypometabolism on ^{18}F-fluorodeoxyglucose (FDG)-PET imaging, previous studies have identified a subset of patients showing a distinct posterior-occipital hypometabolism pattern associated with Lewy body pathology. Here, we aimed to improve the understanding of the clinical relevance of these posterior-occipital FDG-PET patterns in patients with Alzheimer's disease-like amnestic presentations. Our study included 1214 patients with clinical diagnoses of ADD (n = 305) or amnestic mild cognitive impairment (aMCI, n = 909) from the Alzheimer's Disease Neuroimaging Initiative, who had FDG-PET scans available. Individual FDG-PET scans were classified as being suggestive of Alzheimer's (AD-like) or Lewy body (LB-like) pathology by using a logistic regression classifier trained on a separate set of patients with autopsy-confirmed Alzheimer's disease or Lewy body pathology. AD- and LB-like subgroups were compared on amyloid-β and tau-PET, domain-specific cognitive profiles (memory versus executive function performance), as well as the presence of hallucinations and their evolution over follow-up (≈6 years for aMCI, ≈3 years for ADD). Around 12% of the aMCI and ADD patients were classified as LB-like. For both aMCI and ADD patients, the LB-like group showed significantly lower regional tau-PET burden than the AD-like subgroup, but amyloid-β load was only significantly lower in the aMCI LB-like subgroup. LB- and AD-like subgroups did not significantly differ in global cognition (aMCI: d = 0.15, P = 0.16; ADD: d = 0.02, P = 0.90), but LB-like patients exhibited a more dysexecutive cognitive profile relative to the memory deficit (aMCI: d = 0.35, P = 0.01; ADD: d = 0.85 P < 0.001), and had a significantly higher risk of developing hallucinations over follow-up [aMCI: hazard ratio = 1.8, 95% confidence interval = (1.29, 3.04), P = 0.02; ADD: hazard ratio = 2.2, 95% confidence interval = (1.53, 4.06) P = 0.01]. In summary, a sizeable group of clinically diagnosed ADD and aMCI patients exhibit posterior-occipital FDG-PET patterns typically associated with Lewy body pathology, and these also show less abnormal Alzheimer's disease biomarkers as well as specific clinical features typically associated with dementia with Lewy bodies.

1 Unidad de Trastornos del Movimiento, Servicio de Neurología y Neurofisiología Clínica, Instituto de Biomedicina de Sevilla, Hospital Universitario Virgen del Rocío/CSIC/Universidad de Sevilla, 41013 Sevilla, Spain
2 Centro de Investigación Biomédica en Red sobre Enfermedades Neurodegenerativas (CIBERNED), 28029 Madrid, Spain
3 Wallenberg Center for Molecular and Translational Medicine and Department of Psychiatry and Neurochemistry, University of Gothenburg, 41345 Gothenburg, Sweden
4 Dementia Research Centre, Queen Square Institute of Neurology, University College London, WC1E London, UK
5 Departamento de Medicina, Facultad de Medicina, Universidad de Sevilla, 41009 Sevilla, Spain

Correspondence to: Michel Grothe, PhD
Hospital Universitario Virgen del Rocío
Avda. Manuel Siurot, s/n, 41013 Sevilla
E-mail: mgrothe@us.es

Correspondence may also be addressed to: Pablo Mir, MD, PhD
Hospital Universitario Virgen del Rocío
Avda. Manuel Siurot, s/n, 41013 Sevilla
E-mail: pmir@us.es

Introduction

Alzheimer's disease is the most common cause of dementia[1] and is neuropathologically defined by the accumulation of amyloid-β plaques and tau neurofibrillary tangles in the brain. While Alzheimer's disease is typically characterized by a characteristic amnestic dementia syndrome, individual presentations can be highly variable and diagnosing and predicting the course of the disease in the clinic remains challenging.[2] In addition, Alzheimer's disease commonly co-occurs with other pathologies such as Lewy body pathology and TDP-43 inclusions, which can affect the clinical phenotype.[3,4] In a sizeable portion (15–25%) of patients with clinically diagnosed Alzheimer's disease dementia (ADD), these (co-)pathologies can even represent the main pathologic feature (i.e. mimicking Alzheimer's disease clinically).[5,6] Lewy body pathology is typically associated with a distinct clinical syndrome, dementia with Lewy bodies, that is characterized by hallmark diagnostic features such as REM sleep behaviour disorder, visual hallucinations, parkinsonism and cognition fluctuations, in addition to a typically more dysexecutive cognitive profile compared to Alzheimer's disease.[7] In the context of clinical Alzheimer's disease, mixed Alzheimer's disease and Lewy body pathology (AD-LB) has been associated with the development of more clinical features of dementia with Lewy bodies.[8–12] Particularly, the emergence of complex visual hallucinations has been reported to be the most relevant clinical sign of underlying Lewy body neuropathology in clinical Alzheimer's disease.[11]

In the era of disease-modifying therapies, *in vivo* identification of Lewy body (co-)pathology in the context of clinically diagnosed Alzheimer's disease may be critical for clinical patient management, disease prognosis, and clinical trial recruitment. In this regard, PET with the glucose analogue ^{18}F-fluorodeoxyglucose (FDG-PET) is a well established imaging modality for aiding differential dementia diagnosis based on the association of different neurodegenerative pathologies with specific patterns of cerebral hypometabolism.[13,14] Thus, in contrast to the characteristic temporo-parietal pattern of hypometabolism associated with Alzheimer's disease, dementia with Lewy bodies is characterized by a more pronounced posterior-occipital hypometabolism pattern with a relatively spared medial temporal lobe (MTL) and posterior cingulate cortex, the latter being known as the cingulate island sign (CIS).[15–19] In a recent imaging-pathological association study, we observed that a significant subset (12%) of clinical Alzheimer's disease patients actually had a primary pathological diagnosis of Lewy body pathology at autopsy, and these also showed the corresponding posterior-occipital hypometabolism pattern characteristic of dementia with Lewy bodies in ante-mortem FDG-PET.[20] Furthermore, this pattern was also observed in a subset of pathologically mixed AD-LB patients, and was strongly associated with substantia nigra degeneration,[21] which suggests that this posterior-occipital FDG-PET pattern links with Lewy body-related neurodegeneration even in clinical Alzheimer's disease cases.

In the present work we aimed to better understand the clinical relevance of posterior-occipital hypometabolism patterns suggestive of Lewy body pathology among patients with amnestic presentations typical for Alzheimer's disease. We studied the pathological biomarker profiles and clinical trajectories associated to these patterns in a large and well phenotyped cohort of clinically diagnosed patients with amnestic mild cognitive impairment (aMCI) and ADD, and we hypothesized that patients showing such posterior-occipital patterns would show less abnormal Alzheimer's disease biomarker levels as well as more symptomatology characteristic for dementia with Lewy bodies with further disease progression.

Materials and methods

Study participants

Data used in the preparation for this article were obtained from the Alzheimer's Disease Neuroimaging Initiative (ADNI).[22] ADNI was launched in 2003 as a public-private partnership, led by Principal Investigator Michael W. Weiner, MD. The primary goal of ADNI has been to evaluate whether serial MRI, PET, other biological markers, and clinical and neuropsychological assessment can be combined to measure the progression of MCI and early AD. All ADNI studies are conducted according to the Good Clinical Practice guidelines, the Declaration of Helsinki, and U.S. 21 CFR Part 50 (Protection of Human Subjects), and Part 56 (Institutional Review Boards). Written informed consent was obtained from all participants before protocol-specific procedures were performed. The ADNI protocol was approved by the Institutional Review Boards of all of the participating institutions.

Our cohort included 1214 patients from the ADNI with a baseline diagnosis of aMCI ($n = 909$) or ADD ($n = 305$) and at least one FDG-PET image available (henceforth, the 'in vivo cohort') (query date: December 2021). We also made use of data from 28 ADNI patients (five aMCI; 23 ADD) with available FDG-PET images who were followed until death and subjected to neuropathological evaluations following the NIA-AA guidelines for the assessment of Alzheimer's disease and other (often co-morbid) neurodegenerative and cerebrovascular pathologies[23–25] (the 'autopsy cohort'). Standard rating scales for Alzheimer's disease pathology, including Thal amyloid phases, Braak tau stages, and CERAD neuritic plaques, were merged into the Alzheimer's disease neuropathologic change (ADNC) composite score. Assessment of Lewy body pathology followed the McKeith criteria.[7] Patients were considered to have autopsy-confirmed Alzheimer's disease when presenting intermediate or high ADNC,[23] and the presence of Lewy body

neuropathological changes (LBNC) was denoted when Lewy bodies were present in limbic or neocortical regions or the amygdala.[7] Patients with LBNC restricted to the brainstem were excluded. Following these criteria, 21 patients from the autopsy cohort had evidence of Alzheimer's disease pathology without Lewy body co-pathology ('pure-AD'), whereas seven had evidence of Lewy body pathology but no or low Alzheimer's disease pathology ('pure-LB'). A detailed description of the autopsy cohort can be found in our previous publication.[20]

Finally, we also made use of normative FDG-PET data from 179 cognitively normal elderly ADNI participants (the 'control group').

FDG-PET acquisition and processing

FDG-PET images were acquired by using dynamic 3D acquisitions of six 5-min frames starting 30 min after the injection of 185 MBq of FDG. For this work, we used images in preprocessing level four as described by ADNI (adni.loni.usc.edu/methods/pet-analysis-method/pet-analysis/), corresponding to co-registered and averaged images of the six frames standardized and smoothed to a uniform 8 mm isotropic resolution.

FDG-PET images were spatially normalized to the Montreal Neurological Institute (MNI) template space using SPM12 (fil.ion.ucl.ac.uk/spm/software/spm12) and intensity-normalized (to the control group) using a previously validated data-driven method.[26] Volume of interest (VOI) analysis was used for calculating the standardized uptake value ratio (SUVR) of the occipital cortex and the MTL, two regions that have been reported to effectively differentiate between Alzheimer's disease and dementia with Lewy bodies,[19] as well as the well established CIS ratio (CISr), calculated as the ratio between the posterior cingulate cortex uptake and the average of precuneus and cuneus uptake.[15,18,19] The corresponding VOIs were defined using the Harvard-Oxford neuroanatomical atlas (Supplementary Table 1).

Classification of individual FDG-PET patterns from the in vivo cohort

A simple maximum-entropy classification algorithm, also known in machine learning as logistic regression classifier, was trained to distinguish between the FDG-PET signatures from the pure-AD and pure-LB subgroups in the autopsy cohort. The CISr, occipital SUVR, and MTL SUVR data previously derived using the Harvard-Oxford VOIs were used as input parameters. The classifier was implemented using the scikit-learn library (scikit-learn.org). The algorithm was balanced to consider the differences in the number of patients between classes (21 pure-AD versus seven pure-LB). After training, the classifier was applied to the corresponding FDG-PET VOI values from the in vivo cohort. As this kind of logistic classification forces each image into one of the binary output categories and considering that our sample includes a large portion of aMCI patients, patients from the in vivo cohort who did not exhibit any significant hypometabolism were previously filtered. To this end, individual FDG-PET images were transformed to regional z-scores (referenced to the control group) across all the VOIs defined in the Harvard-Oxford atlas, and individuals without notable hypometabolism (defined as $z \leq -1.5$) in any of the relevant brain areas associated with Alzheimer's disease or dementia with Lewy bodies (Supplementary Table 2) were excluded from subsequent analyses. Patients not excluded by this filter were then classified as having FDG-PET patterns suggestive of Alzheimer's disease ('AD-like') or Lewy body pathology ('LB-like') using the neuropathology-trained classifier.

Neuropsychological and neuropsychiatric data

All the patients included in the final cohort had longitudinal cognitive assessment data available (average follow-up: aMCI = 4.3 ± 2.9 years; ADD = 1.7 ± 1.0 years). The Mini-Mental State Examination (MMSE) scores were used for characterizing global cognitive performance,[27] and previously established domain-specific composite scores were used for assessing memory (ADNI-MEM)[28] and executive function (ADNI-EF).[29] In addition, we calculated a 'cognitive profile' variable, Δ(MEM-EF), to characterize the relative impairments between memory and executive function as the difference between z-scored ADNI-MEM and ADNI-EF scores.[30]

Although core features of dementia with Lewy bodies are not specifically assessed in ADNI, participants are longitudinally screened using the Neuropsychiatric Inventory–Questionnaire (NPI-Q),[31] a set of scripted questions administered to the participant's caregivers to evaluate the presence and severity of 12 commonly encountered neuropsychiatric symptoms, including hallucinations. NPI-Q was available for all the patients included in our study group (average follow-up: aMCI = 3.6 ± 2.0; ADD = 1.7 ± 0.9). Patients were considered to have developed hallucinations when the caregivers reported their presence according to the NPI-Q criteria, irrespective of the reported severity. These data were used to assess the emergence of hallucinations over follow-up.

Genetics

APOE genotype was determined by Cogenics using standard methods to genotype the two APOE-ε4-defining single nucleotide polymorphisms (SNPs) (rs429358, rs7412). Patients were labelled as having zero, one, or two ε4 copies.

Amyloid and tau PET

PET scans with radioligands for amyloid-β (Aβ) ([18F]-florbetapir) and tau ([18F]-flortaucipir) were available for 484 (59.8%) and 209 (25.8%) patients of the analysed cohort, respectively. The average time difference (Δt) between FDG- and Aβ-PET acquisitions was Δt = 0.4 ± 1.3 years, while the average time between FDG-PET and tau-PET was Δt = 1.7 ± 1.9 years. As for FDG, Aβ- and tau-PET images were obtained from ADNI at preprocessing level four.

Aβ- and tau-PET images were co-registered to the closest available 3 T anatomical MRI scan (Δt between PET and MRI = 0.1 ± 0.5 years for Aβ; 0.2 ± 0.5 years for tau) using SPM12 and MRI images were segmented using FastSurfer.[32] For Aβ-PET, the subject's parcellation of the Desikan atlas was used for partial volume effect correction (PVC) using the region-based voxel-wise correction (RBV) method[33] as implemented in the open-source PETPVC toolbox.[34] For tau-PET, we used the code shared by Baker et al.[35] for PVC, which also uses the RBV but includes PVC for relevant off-target regions of tau-PET not included in the Desikan atlas.[36] Preprocessed Aβ- and tau-PET images were transformed to SUVR maps by using the whole cerebellum and the lower portion of the cerebellum from the SUIT cerebellar atlas[37] as reference regions, respectively. For voxel-wise analyses, preprocessed images were masked by applying a subject-derived grey matter mask derived from the Desikan grey matter regions, transformed into the MNI space by using the deformation fields obtained from the normalization of the co-registered MRIs and smoothed with a 12-mm Gaussian filter.

In complementary analysis, our voxel-based results were corroborated by using well established region-based metrics. SUVR values were calculated in previously defined global cortical[38] and Braak-stage (I/II, III/IV, V/VI)[39] composite VOIs for Aβ- and tau-PET, respectively. Composite VOIs were constructed by combining the corresponding areas of the Desikan atlas (Supplementary Tables 3 and 4). Amyloid PET positivity was determined by using a threshold of 1.1 SUVR, previously defined for the used VOI-based methodology.[38]

Statistical analysis

Demographic, clinical and biomarker variables were compared using two-sample t-tests for normally distributed continuous variables, Mann-Whitney U-tests for non-normally distributed and ordinal variables, and Fisher's exact tests for categorical variables.

Brain-wide differences between subgroups (AD-like versus LB-like) in Aβ-PET and tau-PET were obtained by performing voxel-wise two-sample t-tests using SPM. Age and sex were used as confounding nuisance covariates. T-score maps were transformed to Cohen's d effect size maps and thresholded using a voxel-level FDR-corrected threshold of $P < 0.05$. To account for possible differences between clinical diagnostic groups, all analyses were assessed separately for aMCI and ADD patients.

Differences in cognitive trajectories between the AD-like and LB-like patient groups were assessed using linear mixed effects models, which included patient-specific intercepts and slopes. Sex, age at baseline, and years of education were used as nuisance covariates for all models. Additionally, models targeting the domain-specific variables ADNI-MEM, ADNI-EF and Δ(MEM-EF), included the MMSE score as a covariate for controlling for global cognition.

Finally, Cox proportional hazard models (lifelines.readthedocs.io) were used for assessing differential risks for developing hallucinations over disease progression. The Breslow estimator was used for obtaining the regression parameters as well as the cumulative baseline hazard function. Age and sex were used as covariates. Cox proportional hazard models were also used to evaluate differential risks of AD-like and LB-like aMCI patients for converting to dementia over follow-up.

Results

Cohort stratification based on logistic regression classifier

The logistic regression classifier achieved an overall accuracy of 87% for separating pure-AD and pure-LB in the autopsy cohort (F1-score = 0.95 for pure-AD, 0.74 for pure-LB). Supplementary Fig. 1 summarizes the classification results of the *in vivo* cohort. Five hundred and twenty-four aMCI (58%) and 285 ADD (93%) patients showed evidence of regional hypometabolism ($z \leq -1.5$) in at least one area relevant to Alzheimer's disease or dementia with Lewy bodies, while 385 aMCI (42%) and 20 ADD (7%) patients were excluded due to the absence of notable hypometabolism in any of these areas. Demographic and clinical information of the excluded patients is presented in Supplementary Table 5. Among the included patients, 111 aMCI (21%) and 38 ADD (13%) patients were classified as presenting an LB-like pattern, while the remaining patients (413 aMCI, 247 ADD) were classified as having an AD-like pattern. Figure 1 presents the FDG-PET hypometabolism patterns of the automatically classified AD-like and LB-like groups. As expected, the classification based on the CISr, MTL SUVR, and occipital SUVR

was effective in separating between patients with AD-like temporo-parietal hypometabolism patterns and patients with LB-like posterior-occipital hypometabolism patterns. Additional information about regional SUVRs is reported in Supplementary Fig. 2.

Table 1 summarizes demographical and clinical data at baseline. No differences between groups were found for age, sex, years of education, or APOE-ε4 positivity. Regarding baseline cognition, global cognition as measured by the MMSE was similar between groups. However, LB-like aMCI patients exhibited a significantly less pronounced memory deficit than AD-like aMCI patients ($d = 0.50$, $P < 0.001$) but a similar executive function deficit. These differences resulted in a more executive-predominant cognitive profile in the LB-like compared to the AD-like group as assessed by the Δ(MEM-EF) variable ($d = 0.35$, $P = 0.01$). Accordingly, clinicians tended to assign a diagnosis of 'MCI due to Alzheimer's disease' (in contrast to 'MCI due to other aetiologies') more frequently in the AD-like group (91%) than in the LB-like group (82%) ($P = 0.07$). In the ADD group, LB-like patients exhibited similar memory deficits when compared to AD-like patients, but more severe executive dysfunctions ($d = -0.59$, $P < 0.001$), which together also resulted in a more executive-predominant cognitive profile in the LB-like compared to the AD-like group (Δ(MEM-EF): $d = 0.85$, $P < 0.001$).

Alzheimer's disease pathological profiles

For aMCI patients, voxel-wise SPM analysis revealed a significantly lower Aβ uptake across widespread neocortical regions in LB-like compared to AD-like patients (Fig. 2). These differences were not observed for ADD, where voxel-wise maps revealed similar Aβ load between the LB-like and AD-like groups across the whole brain. VOI-based analysis (Supplementary Fig. 3) corroborated the voxel-wise findings, with a significantly lower cortical composite SUVR for the LB-like versus AD-like group in aMCI ($d = -0.43$, $P = 0.002$, 58% versus 70% amyloid-positive) but not in ADD ($d = 0.03$, $P = 0.89$, 88% versus 90% amyloid-positive).

Regarding tau-PET, aMCI patients in the LB-like group showed significantly lower tau load than those in the AD-like group, especially noticeable in regions where tau accumulation is typically observed in Alzheimer's disease, including the medial, inferior and lateral temporal lobe, the posterior cingulate, frontal and inferior parietal regions (Fig. 3). Similarly, in ADD the LB-like patients also showed significantly lower tau load compared to the AD-like group, which was however most noticeable in frontal and lateral temporal regions rather than in medial temporal and parietal regions. Interestingly, occipital tau load did not significantly differ between the groups and in ADD was even numerically higher in the LB-like group. In accordance with the voxel-wise findings, VOI-based analyses (Supplementary Fig. 4) showed significantly lower tau load in the LB-like versus AD-like groups across all Braak composite VOIs in aMCI (Braak I/II: $d = -1.08$, $P < 0.001$; Braak III/IV: $d = -0.86$, $P < 0.001$; Braak V/VI: $d = -0.74$, $P = 0.004$), but only in Braak III/IV ($d = -0.91$, $P = 0.04$) and Braak V/VI ($d = -0.93$, $P = 0.03$) VOIs in ADD (Braak I/II: $d = -0.52$, $P = 0.23$).

Clinical follow-up

In longitudinal clinical follow-up, linear mixed effects models revealed that LB-like patients in the aMCI group showed a significantly slower global cognitive decline (MMSE: $d = -0.28$, $P = 0.011$) compared to AD-like patients, which was mainly driven by a slower memory decline (ADNI-MEM: $d = -0.39$, $P = 0.002$), while executive function decline was similar between groups (ADNI-EF: $d = -0.14$,
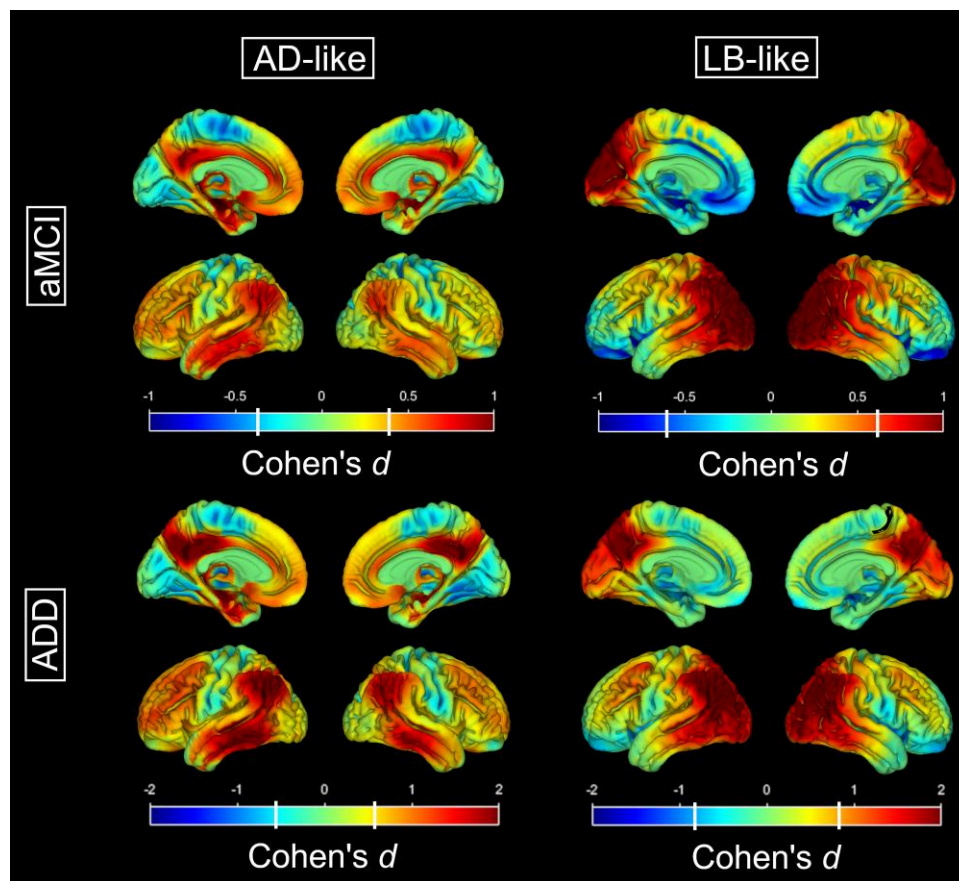
Figure 1 Differential hypometabolism patterns for the AD-like and the LB-like patients. Hypometabolism patterns (as compared to the healthy control group) for the AD-like (*left*) and LB-like (*right*) groups stratified by aMCI (*top*) and ADD (*bottom*). Colour scales represent effect size (Cohen's *d*), and white vertical bars in the colour scale denote the effect size corresponding to a statistical threshold of P (FDR) < 0.05. AD = Alzheimer's disease; ADD = Alzheimer's disease dementia; aMCI = amnestic mild cognitive impairment; LB = Lewy body.

$P = 0.90$) (Fig. 4, top). As a result, the aMCI LB-like patients progressed towards a more executive-predominant cognitive profile over time, while AD-like patients remained stable in a relatively balanced profile [Δ(MEM-EXEC): $d = 0.31$, $P = 0.002$]. Regarding neuropsychiatric symptoms, survival analysis revealed that aMCI patients in the LB-like group had a significantly higher risk of developing hallucinations over time: 27% of the LB-like patients developed hallucinations over follow-up, compared to 16% in the AD-like group [hazard ratio (HR) = 1.8, 95% confidence interval (CI) = (1.29, 3.04), $P = 0.02$] (Fig. 5, left). In line with the slower cognitive decline, LB-like aMCI patients were also less likely to progress to a diagnosis of dementia over follow-up [27% versus 44%, HR = 0.53, 95% CI = (0.4, 0.67), $P < 0.005$; Supplementary Fig. 5]. Interestingly, ADD was the most common clinical diagnosis for converters in both the AD-like and LB-like groups, where only 9% and 7%, respectively, were clinically judged to be of 'other aetiologies' (which were not further specified in the ADNI documentation). However, converters in the AD-like group were more likely to receive a confident diagnosis of 'probable Alzheimer's disease' (86% versus 73%, $P = 0.09$), whereas converters in the LB-like group were comparably more often diagnosed with 'possible Alzheimer's disease' (20% versus 5%, $P = 0.01$).

In the ADD group, we did not observe any differences in global cognitive decline between the AD-like and LB-like patients (MMSE: $d = -0.09$, $P = 0.82$), nor in memory decline (ADNI-MEM:

$d = -0.12$, $P = 0.73$) (Fig. 4, bottom). However, in contrast to aMCI, in ADD the LB-like group's executive performance declined significantly slower than in the AD-like group (ADNI-EF: $d = -0.38$, $P = 0.04$). As a result, LB-like ADD patients evolved from a more executive-predominant to a more balanced cognitive profile over follow-up, whereas AD-like patients again remained stable in a relatively balanced profile [Δ(MEM-EXEC): $d = 0.32$, $P = 0.07$]. Interestingly, LB-like ADD patients also had a significantly higher risk of developing hallucinations over follow-up compared to the AD-like patients [60% and 30%, respectively; HR = 2.2, 95% CI = (1.53, 4.06) $P = 0.01$] (Fig. 5, right).

Discussion

To better understand the relevance of FDG-PET findings suggestive of underlying Lewy body pathology in the context of a clinical Alzheimer's disease phenotype, we analysed individual FDG-PET patterns in a large cohort of more than 1200 aMCI and ADD patients. Compared to patients with a temporo-parietal FDG-PET pattern typical for Alzheimer's disease, patients with a posterior-occipital FDG-PET pattern showed less Alzheimer's disease biomarker burden in PET imaging, as well as specific clinical features typically associated with dementia with Lewy bodies, such as a more dysexecutive cognitive profile and a higher risk of developing hallucinations over follow-up.

Table 1 Demographic and clinical data for the different study groups

	aMCI (n = 524)			ADD (n = 285)		
	AD-like (n = 413)	LB-like (n = 111)	AD-like versus LB-like	AD-like (n = 247)	LB-like (n = 38)	AD-like versus LB-like
Age, years	74.6 ± 6.9	73.4 ± 8.2	d = −0.21 P = 0.12	75.2 ± 8.1	75.0 ± 7.5	d = −0.02 P = 0.87
Male/female, %	60/40	65/35	P = 0.38	61/39	58/42	P = 0.72
Education, years	16.0 ± 2.7	16.3 ± 2.7	d = 0.10 P = 0.34	15.4 ± 2.8	15.2 ± 2.5	d = −0.09 P = 0.59
APOE ε4, −−/+−/++, %	49/40/11	51/39/10	P = 0.91	32/47/21	37/49/14	P = 0.70
MMSE	27.4 ± 1.9	27.7 ± 1.6	d = 0.15 P = 0.16	23.1 ± 2.2	23.1 ± 2.7	d = 0.02 P = 0.90
ADNI-MEM	0.0 ± 0.6	0.4 ± 0.7	d = 0.50 P < 0.001[a]	−0.9 ± 0.5	−0.8 ± 0.5	d = 0.22 P = 0.21
ADNI-EF	0.1 ± 0.9	0.2 ± 0.9	d = 0.14 P = 0.17	−0.9 ± 0.9	−1.5 ± 0.9	d = −0.59 P < 0.001[a]
Δ(MEM-EF)	0.0 ± 0.8	0.3 ± 0.8	d = 0.35 P = 0.01[a]	−0.26 ± 0.8	0.46 ± 0.8	d = 0.85 P < 0.001[a]

Patients are grouped by clinical diagnosis (aMCI versus ADD) and by FDG-PET classification (AD-like versus LB-like). AD = Alzheimer's disease; ADD = Alzheimer's disease dementia; aMCI = amnestic mild cognitive impairment; LB = Lewy body; MMSE = Mini-Mental State Examination; MEM = memory; EF = executive function.
[a]Significantly different at P < 0.05 when compared to the AD-like group.

According to our classification, 12.2% of the whole aMCI cohort and 12.5% of the ADD cohort showed a posterior-occipital FDG-PET pattern suggestive of Lewy body pathology. While these percentages are in good agreement with the proportion of clinical Alzheimer's disease cases in the ADNI autopsy cohort who were found to have a primary pathological diagnosis of Lewy body pathology,[20,40] they are higher than those reported by previous neuropathological studies focusing on similar clinical Alzheimer's disease cohorts (3–11%).[41,42] According to our previous imaging-pathological study,[20] several of the LB-like cases in our study may actually reflect pathologically mixed AD-LB cases for which Lewy body pathology represents an important contribution to the neurodegeneration phenotype, which may explain the relatively large size of our LB-like group. Although the actual underlying pathology in the FDG-PET-defined LB-like patients in our current study remains unknown, these patients did indeed show significantly lower PET biomarker levels of Alzheimer's disease pathology compared to patients with an AD-like FDG-PET pattern, indicating that co-pathologies may have a greater contribution to the clinical phenotype. While in aMCI the LB-like group showed both significantly lower Aβ load and tau burden compared to the AD-like group, in ADD the LB-like group showed significantly lower regional tau burden but similar Aβ load compared to AD-like patients. Tau burden was particularly lower in frontal and lateral temporo-parietal areas, suggesting a less advanced stage of regional tau progression in these patients.[43] Interestingly, LB-like patients showed a comparatively high occipital tau burden when compared to other neocortical regions (e.g. frontal, posterior cingulate), a pattern that was also observed in previous tau-PET studies evaluating patients clinically diagnosed with dementia with Lewy bodies.[44,45] Altogether, the relatively high amyloid burden in combination with the significantly lower but non-negligible tau pathology in the LB-like cases indicates that several of these cases have at least some degree of Alzheimer's disease pathology that is contributing to their phenotype. However, in light of the characteristic posterior-occipital FDG-PET pattern and the mixed clinical phenotype that characterizes the LB-like cases in our study, it appears likely that these patients may have a greater contribution of (comorbid) LB pathology to their neurodegeneration phenotype and associated clinical features.[20] Of note, a very similar posterior-occipital FDG-PET hypometabolism pattern has also been reported in patients with posterior cortical atrophy, and thus some of the classified LB-like patients may also reflect such a rare, atypical subtype of Alzheimer's disease.[46] Posterior cortical atrophy typically presents as a form of early onset Alzheimer's disease (EOAD, < 65 years), so our results may not directly translate to younger populations where the proportion of patients with posterior cortical atrophy and other forms of EOAD is expected to be higher.[47]

Irrespective of the possible underlying neuropathological characteristics, the patients classified as LB-like in our study showed distinct clinical trajectories compatible with a mixed AD-LB clinical profile, thus emphasizing the clinical relevance of this hypometabolic pattern even in the absence of core clinical features of dementia with Lewy bodies.[7] When compared to the AD-like group, LB-like patients exhibited a significantly more dysexecutive cognitive profile, characteristic for dementia with Lewy bodies,[48–50] which was driven by a relatively less impaired memory performance at early stages (aMCI) and by a more pronounced executive deficit in ADD. Most importantly, these differences were observed at comparable levels of global cognitive impairment (MMSE), which suggests that these domain-specific differences represent in fact different cognitive profiles instead of different stages of disease progression. Over clinical follow-up, pre-demented LB-like patients evolved towards an even more dysexecutive profile, mainly driven by a relatively slower memory compared to executive function decline. However, this was not observed for ADD, where LB-like patients evolved from a more dysexecutive profile to a more balanced profile over time. This could be partly explained by the marked severity of executive deficits already at baseline in the LB-like ADD patients, such that the subsequent cognitive decline is measured mainly in the memory domain.[51] Interestingly, both in the aMCI and ADD groups, LB-like patients were at a significantly higher risk of developing hallucinations over follow-up. While such neuropsychiatric symptoms can arise in all forms of dementia, a markedly higher prevalence has been reported in dementia with Lewy bodies compared to other dementia types,[52,53] and visual hallucinations have been reported to be among the most relevant clinical features to distinguish between autopsy-confirmed Alzheimer's disease and dementia with Lewy bodies,[54] and also between dementia with Lewy bodies and posterior cortical atrophy.[55] A clinico-pathological study on clinically diagnosed ADD cases further showed that the presence of visual hallucinations was a strong clinical predictor of (comorbid) Lewy body neuropathology.[11]

While longitudinal global cognitive decline as measured by MMSE was similar between both ADD groups, aMCI LB-like patients declined significantly slower than aMCI AD-like patients. This was
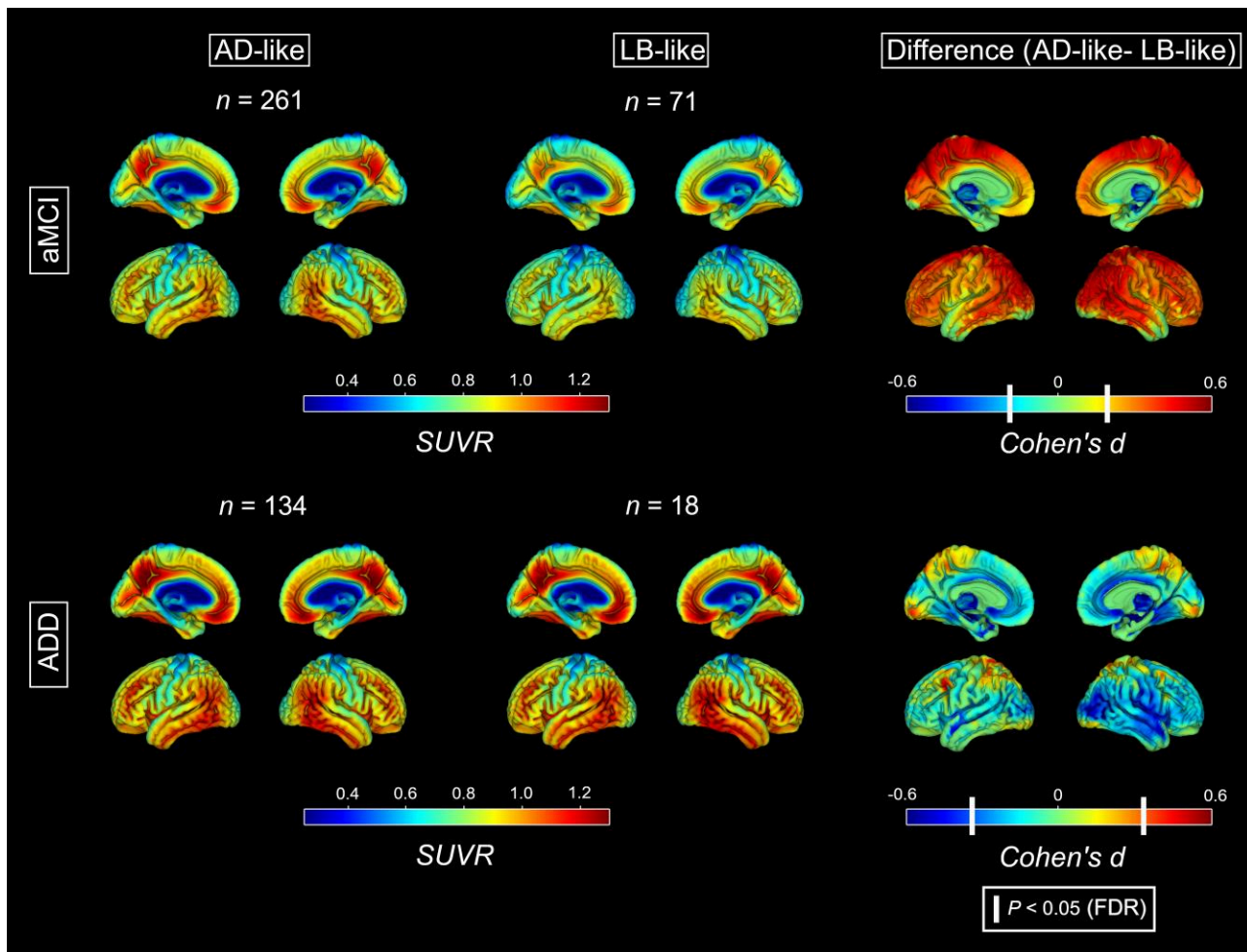
Figure 2 Amyloid deposition maps for the AD-like and the LB-like groups. Standardized uptake value ratio (SUVR) maps of amyloid deposition calculated from Aβ-PET for the AD-like (*left*) and LB-like (*centre*) groups, stratified by aMCI (*top*) and ADD (*bottom*). *Right*: The voxel-wise analyses contrasting the AD-like and LB-like groups. White vertical bars in the Cohen's *d* colour scales denote the effect sizes corresponding to a statistical threshold of *P* (FDR) < 0.05. AD = Alzheimer's disease; ADD = Alzheimer's disease dementia; aMCI = amnestic mild cognitive impairment; LB = Lewy body.

also observed in the conversion to dementia, where AD-like aMCI patients were almost twice as likely to progress to dementia compared to LB-like patients (HR = 0.53). These results contrast with recent reports from autopsy cohorts suggesting a faster clinical decline in dementia with Lewy bodies and mixed AD-LB compared to Alzheimer's disease.[56,57] However, in both cases the studied cohorts included clinically diagnosed dementia with Lewy bodies and Alzheimer's disease patients, while our cohort is composed only of patients with a clinical Alzheimer's disease phenotype. Interestingly, Hamilton *et al.*[57] also reported that clinical decline increased as a function of the observed core features of dementia with Lewy bodies, and these were completely absent in our cohort (at baseline). Further studies are warranted to investigate in more detail the commonalities and differences between the FDG-PET-defined LB-like aMCI patients in our study and patients clinically diagnosed as MCI due to prodromal dementia with Lewy bodies.[7] With respect to the clinical dementia profile, dementia converters in the LB-like group were more likely to receive a clinical diagnosis of 'possible' instead of 'probable' Alzheimer's disease, probably reflecting the higher proportion of atypical clinical features (more dysexecutive cognitive profile, presence of hallucinations) in this group. However, clinical diagnoses of 'other

dementia' aetiologies were equally rare in both groups (9% versus 7%). Thus, although many of these converted aMCI patients would present with at least one core feature of dementia with Lewy bodies (hallucinations) and a supportive biomarker (FDG-PET pattern), their overall clinical features are probably insufficient to meet full diagnostic criteria for 'possible dementia with Lewy bodies' according to current guidelines.[58] In addition, it is possible that dementia with Lewy bodies is underdiagnosed in the Alzheimer's disease-focussed ADNI study.

Taken together, our results revealed that a posterior-occipital hypometabolism pattern suggestive of underlying Lewy body pathology is clinically relevant in the context of clinical Alzheimer's disease, being associated with lower Alzheimer's disease pathology, a more dysexecutive cognitive profile, and a higher risk of developing hallucinations over time. These findings add further evidence to the utility of pathology-specific FDG-PET patterns for predicting the clinical course of patients even at pre-dementia stages,[13,59,60] and suggest that these FDG-PET hallmarks should be considered for clinical management even in the absence of any core clinical features of dementia with Lewy bodies. The degree to which the patients with an LB-like FDG-PET pattern actually exhibit (comorbid) Lewy body pathology remains unknown in our study and
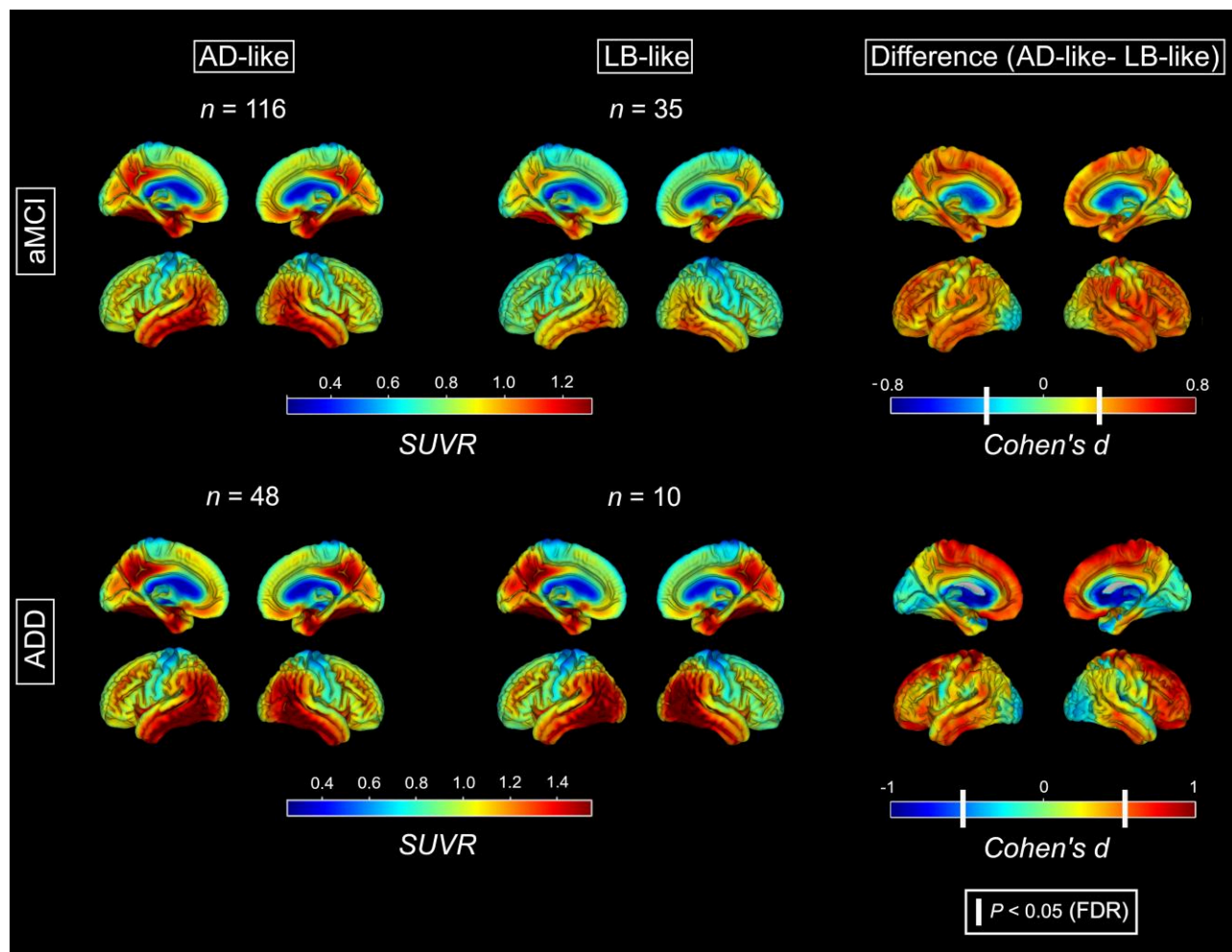
Figure 3 Tau deposition maps for the AD-like and the LB-like groups. Standardized uptake value ratio (SUVR) maps of tau deposition calculated from tau-PET for the AD-like (*left*) and LB-like (*centre*) groups, stratified by aMCI (*top*) and ADD (*bottom*). *Right*: The voxel-wise analyses contrasting the AD-like and the LB-like groups. White vertical bars in the Cohen's *d* colour scale denote the effect size corresponding to a statistical threshold of *P* (FDR) < 0.05.

represents an important venue for further research. In our recent imaging-pathological association study,[20] we found that the posterior-occipital FDG-PET pattern was not related to the presence of Lewy body pathology by itself, but rather to associated substantia nigra degeneration.[21] Future studies may assess the degree of dopaminergic degeneration in these *in vivo* classified LB-like patients. In addition to a better characterization of the actual pathological characteristics of the FDG-PET-defined LB-like cases, future studies are warranted to assess whether these patients also show some of the pharmacological characteristics associated with dementia with Lewy bodies, such as a higher susceptibility to antagonistic dopaminergic neuroleptics and a generally better response to treatment with acetylcholinesterase inhibitors,[61] which may be of paramount importance for clinical patient management and clinical trial recruitment.[62]

Our work presents a series of limitations. First, our logistic classifier has a binary output, so it is likely that our groups still represent a high degree of heterogeneity, especially the AD-like group. Concretely, our AD-like group likely presents a mixture of different Alzheimer's disease subtypes as identified previously using data-driven approaches,[30] and may also include patients with patterns reflective of other common age-related pathologies

targeting the medial temporal lobe, such as limbic age-related TDP-43 encephalopathy (LATE).[59] Furthermore, despite being trained in autopsy-based data, our classifier did not achieve perfect performance in distinguishing between the pure-AD and the pure-LB groups. Particularly, our algorithm did an excellent work in identifying the pure-AD cases (F1-score = 0.95), but the performance was lower for identifying pure-LB cases (F1-score = 0.74). These differences in performance may be related to the relatively small size of the pure-LB group (*n* = 7) and may have potentially resulted in an underestimation of the size of the classified LB-like group. Regarding clinical assessments, neuropsychologic data collected within the ADNI study allow for the assessment of specific (dysexecutive versus amnestic-predominant) neuropsychological profiles, but core features of dementia with Lewy bodies are not systematically assessed in enough detail (or, except for hallucinations, not assessed at all). Regarding the assessment of hallucinations, while the NPIQ is a widely accepted instrument, more sophisticated metrics to assess the type and nature of hallucinations have been developed and could have provided more detailed insights into the heightened hallucination risk in the LB-like group.[63] Concretely, NPIQ data do not provide a separated item for visual hallucinations, which would have been a better representation of
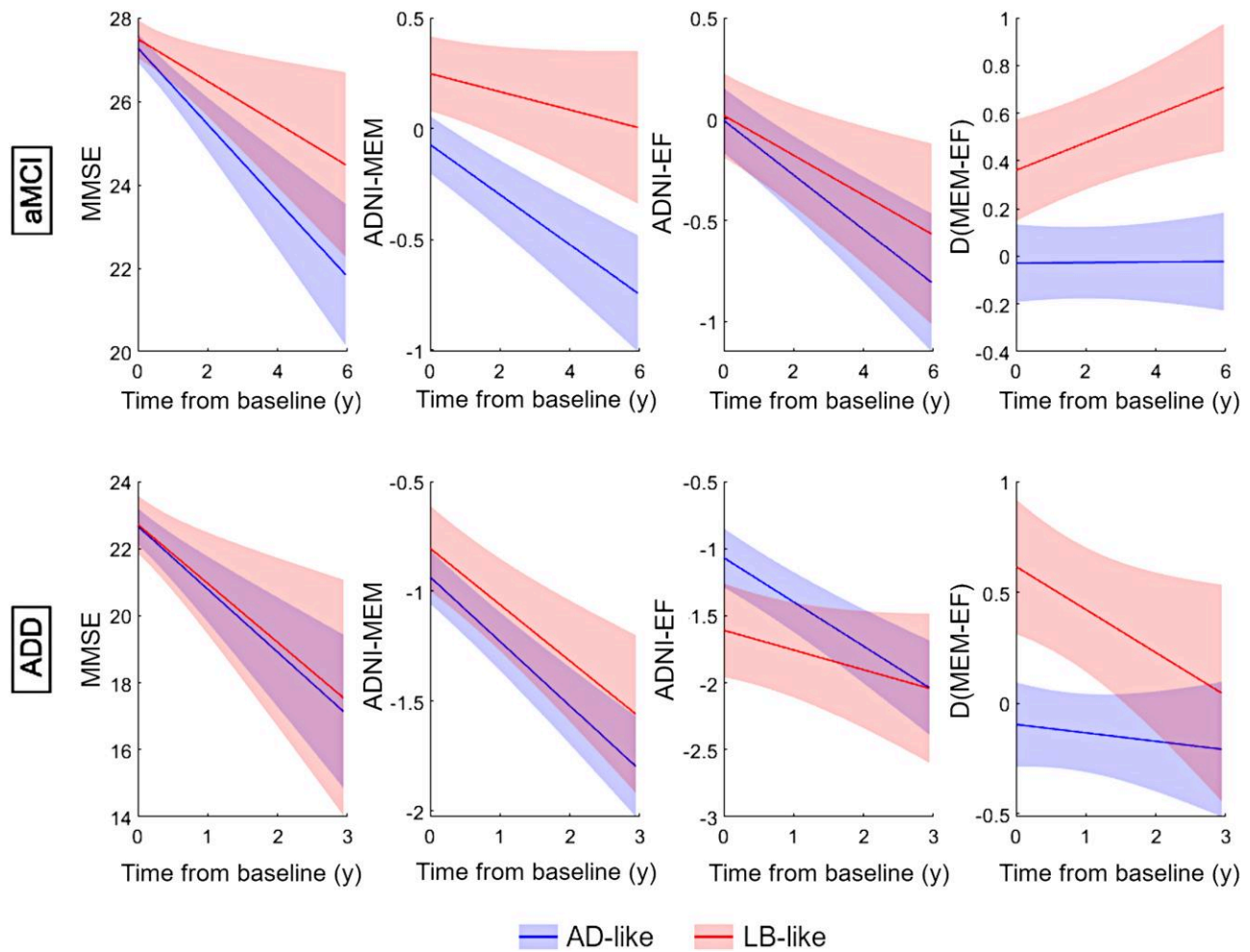
Figure 4 Differential cognitive trajectories for the AD-like and LB-like groups. Estimated cognitive trajectories of MMSE (*left*), ADNI-MEM (*centre-left*), ADNI-EF (*centre-right*) and cognitive profile Δ(MEM-EF) (*right*) for subjects within the AD-like (blue line) and LB-like groups (red line), stratified by aMCI (*top*) and ADD (*bottom*). Group trajectories were estimated using covariate-adjusted linear mixed models with subject-specific intercepts. EF = executive function; MEM = memory; MMSE = Mini-Mental State Examination.
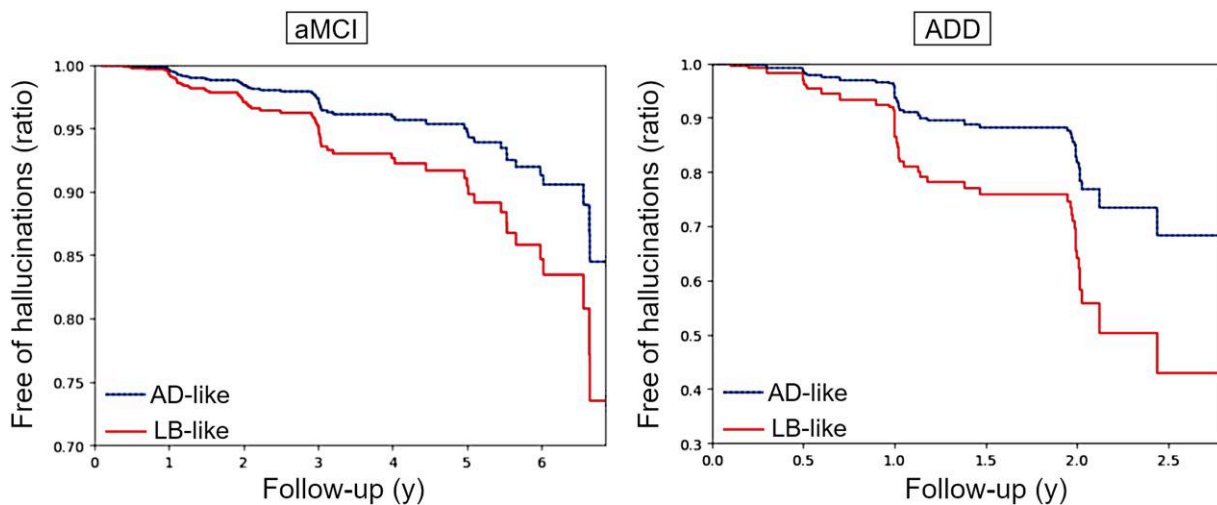
Figure 5 Development of hallucinations over follow-up. Predicted proportions of subjects remaining free of hallucinations according to the fitted Cox proportional hazard models for subjects within the AD-like (blue line) and LB-like (red line) groups, stratified by aMCI (*left*) and ADD (*right*). Models were fitted independently for aMCI and ADD. AD = Alzheimer's disease; ADD = Alzheimer's disease dementia; aMCI = amnestic mild cognitive impairment; LB = Lewy body.

the type of hallucinations typically observed in dementia with Lewy bodies. Finally, despite the large size of the cohort, the number of LB-like ADD patients with available amyloid ($n = 18$) and tau PET ($n = 10$) scans was small, so our biomarker results should be confirmed by further studies.

In summary, our study showed that a sizeable group of elderly patients with amnestic presentations typical for Alzheimer's disease exhibits a posterior-occipital hypometabolism pattern typically linked to Lewy body pathology, and this associates with lower Alzheimer's disease biomarker burden, a distinctive dysexecutive cognitive profile, and a higher risk of developing hallucinations over time. This may have important implications for both clinical patient management and Alzheimer's disease clinical trial recruitment. In the clinic, patients showing this differential hypometabolism pattern should be subjected to special consideration even without any *a priori* clinical suspicion of underlying Lewy body pathology.

Data availability

All patient data used in the preparation of this article are available through the Alzheimer's Disease Neuroimaging Initiative (ADNI) database (adni.loni.usc.edu). The processed datasets generated and/or analysed in the current study are available from the corresponding author upon reasonable request.

Acknowledgements

Data used in preparation of this article were obtained from the Alzheimer's Disease Neuroimaging Initiative (ADNI) database (http://adni.loni.usc.edu/). As such, the investigators within the ADNI contributed to the design and implementation of ADNI and/or provided data but did not participate in analysis or writing of this report. A complete listing of ADNI investigators can be found at: http://adni.loni.usc.edu/wp-content/uploads/how_to_apply/ADNI_Acknowledgement_List.pdf

Funding

Competing interests

J.S.R. is a founder and advisor for Qubiotech Health Intelligence SL, a company commercializing neuroimaging quantification software.

Supplementary material

Supplementary material is available at *Brain* online.

References

1. 2021 Alzheimer's disease facts and figures. *Alzheimers Dement*. 2021;17:327-406.
2. Birkenbihl C, Salimi Y. Fröhlich H. Unraveling the heterogeneity in Alzheimer's disease progression across multiple cohorts and the implications for data-driven disease modeling. *Alzheimers Dement*. 2022;18:251-261.
3. Robinson JL, Richardson H, Xie SX, *et al*. The development and convergence of co-pathologies in Alzheimer's disease. *Brain J Neurol*. 2021;144:953-962.
4. Tomé SO, Thal DR. Co-pathologies in Alzheimer's disease: Just multiple pathologies or partners in crime? *Brain*. 2021;144: 706-708.
5. Auning E, Rongve A, Fladby T, *et al*. Early and presenting symptoms of dementia with Lewy bodies. *Dement Geriatr Cogn Disord*. 2011;32:202-208.
6. Beach TG, Monsell SE, Phillips LE, Kukull W. Accuracy of the clinical diagnosis of Alzheimer disease at national institute on aging Alzheimer disease centers, 2005–2010. *J Neuropathol Exp Neurol*. 2012;71:266-273.
7. McKeith IG, Boeve BF, Dickson DW, *et al*. Diagnosis and management of dementia with Lewy bodies: Fourth consensus report of the DLB consortium. *Neurology*. 2017;89:88-100.
8. Chatterjee A, Hirsch-Reinshagen V, Moussavi SA, Ducharme B, Mackenzie IR, Hsiung GR. Clinico-pathological comparison of patients with autopsy-confirmed Alzheimer's disease,

dementia with Lewy bodies, and mixed pathology. *Alzheimers Dement Diagn Assess Dis Monit.* 2021;13.

9. Brenowitz WD, Hubbard RA, Keene CD, *et al.* Mixed neuro-pathologies and associations with domain-specific cognitive decline. *Neurology.* 2017;89:1773-1781.

10. Savica R, Beach TG, Hentz JG, *et al.* Lewy Body pathology in Alzheimer's disease: A clinicopathological prospective study. *Acta Neurol Scand.* 2019;139:76-81.

11. Thomas AJ, Mahin-Babaei F, Saidi M, *et al.* Improving the identification of dementia with Lewy bodies in the context of an Alzheimer's-type dementia. *Alzheimers Res Ther.* 2018;10:27.

12. Azar M, Chapman S, Gu Y, Leverenz JB, Stern Y, Cosentino S. Cognitive tests aid in clinical differentiation of Alzheimer's disease versus Alzheimer's disease with Lewy body disease: Evidence from a pathological study. *Alzheimers Dement J Alzheimers Assoc.* 2020;16:1173-1181.

13. Arbizu J, Festari C, Altomare D, *et al.* Clinical utility of FDG-PET for the clinical diagnosis in MCI. *Eur J Nucl Med Mol Imaging.* 2018;45:1497-1508.

14. Nestor PJ, Altomare D, Festari C, *et al.* Clinical utility of FDG-PET for the differential diagnosis among the main forms of dementia. *Eur J Nucl Med Mol Imaging.* 2018;45:1509-1525.

15. Kantarci K, Boeve BF, Przybelski SA, *et al.* FDG PET metabolic signatures distinguishing prodromal DLB and prodromal AD. *Neuroimage Clin.* 2021;31:102754.

16. Kondo D, Ota K, Kasanuki K, *et al.* Characteristics of mild cognitive impairment tending to convert into Alzheimer's disease or dementia with Lewy bodies: A follow-up study in a memory clinic. *J Neurol Sci.* 2016;369:102-108.

17. Lim SM, Katsifis A, Villemagne VL, *et al.* The 18 F-FDG PET cingulate island sign and comparison to ^{123} I-β-CIT SPECT for diagnosis of dementia with Lewy bodies. *J Nucl Med.* 2009;50:1638-1645.

18. Graff-Radford J, Murray ME, Lowe VJ, *et al.* Dementia with Lewy bodies: Basis of cingulate island sign. *Neurology.* 2014;83:801-809.

19. Gjerum L, Frederiksen KS, Henriksen OM, *et al.* Evaluating 2-[18F]FDG-PET in differential diagnosis of dementia using a data-driven decision model. *Neuroimage Clin.* 2020;27:102267.

20. Silva-Rodríguez J, Labrador-Espinosa MA, Moscoso A, *et al.* Differential effects of tau stage, Lewy body pathology, and substantia nigra degeneration on FDG-PET patterns in clinical Alzheimer disease. *J Nucl Med* 2023;64:274–280.

21. Seidel K, Mahlke J, Siswanto S, *et al.* The brainstem pathologies of Parkinson's disease and dementia with Lewy bodies. *Brain Pathol.* 2015;25:121-135.

22. Mueller SG, Weiner MW, Thal LJ, *et al.* The Alzheimer's disease neuroimaging initiative. *Neuroimaging Clin N Am.* 2005;15:869-877, xi-xii.

23. Montine TJ, Phelps CH, Beach TG, *et al.* National Institute on Aging–Alzheimer's Association guidelines for the neuropathologic assessment of Alzheimer's disease: A practical approach. *Acta Neuropathol.* 2012;123:1-11.

24. Hyman BT, Phelps CH, Beach TG, *et al.* National institute on aging–Alzheimer's association guidelines for the neuropathologic assessment of Alzheimer's disease. *Alzheimers Dement.* 2012;8:1-13.

25. Franklin EE, Perrin RJ, Vincent B, *et al.* Brain collection, standardized neuropathologic assessment, and comorbidity in Alzheimer's disease neuroimaging initiative 2 participants. *Alzheimers Dement.* 2015;11:815-822.

26. López-González FJ, Silva-Rodríguez J, Paredes-Pacheco J, *et al.* Intensity normalization methods in brain FDG-PET quantification. *Neuroimage* 2020;222:117229.

27. Balsis S, Benge JF, Lowe DA, Geraci L, Doody RS. How do scores on the ADAS-cog, MMSE, and CDR-SOB correspond? *Clin Neuropsychol.* 2015;29:1002-1009.

28. Crane PK, Carle A, Gibbons LE, *et al.* Development and assessment of a composite score for memory in the Alzheimer's disease neuroimaging initiative (ADNI). *Brain Imaging Behav.* 2012;6:502-516.

29. Gibbons LE, Carle AC, Mackin RS, *et al.* A composite score for executive functioning, validated in Alzheimer's disease neuroimaging initiative (ADNI) participants with baseline mild cognitive impairment. *Brain Imaging Behav.* 2012;6:517-527.

30. Levin F, Ferreira D, Lange C, *et al.* Data-driven FDG-PET subtypes of Alzheimer's disease-related neurodegeneration. *Alzheimers Res Ther.* 2021;13:49.

31. Cummings JL, Mega M, Gray K, Rosenberg-Thompson S, Carusi DA, Gornbein J. The neuropsychiatric inventory: Comprehensive assessment of psychopathology in dementia. *Neurology.* 1994;44:2308-2308.

32. Henschel L, Conjeti S, Estrada S, Diers K, Fischl B, Reuter M. Fastsurfer - A fast and accurate deep learning based neuroimaging pipeline. *Neuroimage.* 2020;219:117012.

33. Hutton BF, Thomas BA, Erlandsson K, *et al.* What approach to brain partial volume correction is best for PET/MRI? *Nucl Instrum Methods Phys Res Sect Accel Spectrometers Detect Assoc Equip.* 2013;702:29-33.

34. Thomas BA, Cuplov V, Bousse A, *et al.* PETPVC: A toolbox for performing partial volume correction techniques in positron emission tomography. *Phys Med Biol.* 2016;61:7975-7993.

35. Baker SL, Maass A, Jagust WJ. Considerations and code for partial volume correcting [18F]-AV-1451 tau PET data. *Data Brief.* 2017;15:648-657.

36. López-González FJ, Costoya-Sánchez A, Paredes-Pacheco J, Moscoso A, Silva-Rodríguez J, Aguiar P. Impact of spill-in counts from off-target regions on [18F]flortaucipir PET quantification. *Neuroimage.* 2022;259:119396.

37. Diedrichsen J, Balsters JH, Flavell J, Cussans E, Ramnani N. A probabilistic MR atlas of the human cerebellum. *Neuroimage.* 2009;46:39-46.

38. Landau SM, Breault C, Joshi AD, *et al.* Amyloid-β imaging with Pittsburgh compound B and florbetapir: Comparing radiotracers and quantification methods. *J Nucl Med.* 2013;54:70-77.

39. Lemoine L, Leuzy A, Chiotis K, Rodriguez-Vieitez E, Nordberg A. Tau positron emission tomography imaging in tauopathies: The added hurdle of off-target binding. *Alzheimers Dement (Amst).* 2018;10:232-236.

40. Mohanty R, Ferreira D, Frerich S, *et al.* Neuropathologic features of antemortem atrophy-based subtypes of Alzheimer disease. *Neurology* 2022;99:e323–e333.

41. Middleton LE, Grinberg LT, Miller B, Kawas C, Yaffe K. Neuropathologic features associated with Alzheimer disease diagnosis: Age matters. *Neurology.* 2011;77:1737-1744.

42. Gauthreaux K, Bonnett TA, Besser LM, *et al.* Concordance of clinical Alzheimer diagnosis and neuropathological features at autopsy. *J Neuropathol Exp Neurol.* 2020;79:465-473.

43. Schöll M, Lockhart SN, Schonhaut DR, *et al.* PET Imaging of tau deposition in the aging human brain. *Neuron.* 2016;89:971-982.

44. Kantarci K, Lowe VJ, Boeve BF, *et al.* AV-1451 tau and β-amyloid positron emission tomography imaging in dementia with Lewy bodies. *Ann Neurol.* 2017;81:58-67.

45. Day GS, Gordon BA, Jackson K, *et al.* Tau-PET binding distinguishes patients with early-stage posterior cortical atrophy from amnestic Alzheimer disease dementia. *Alzheimer Dis Assoc Disord.* 2017;31:87-93.

46. Whitwell JL, Graff-Radford J, Singh TD, *et al.* 18F-FDG PET in posterior cortical atrophy and dementia with Lewy bodies. *J Nucl Med.* 2017;58:632-638.

47. Chiari A, Vinceti G, Adani G, *et al*. Epidemiology of early onset dementia and its clinical presentations in the province of Modena, Italy. *Alzheimers Dement*. 2021;17:81-88.

48. Brønnick K, Breitve MH, Rongve A, Aarsland D. Neurocognitive deficits distinguishing mild dementia with Lewy bodies from mild Alzheimer's disease are associated with parkinsonism. *J Alzheimers Dis*. 2016;53:1277-1285.

49. Goldman JG, Williams-Gray C, Barker RA, Duda JE, Galvin JE. The spectrum of cognitive impairment in Lewy body diseases. *Mov Disord*. 2014;29:608-621.

50. Ferman TJ, Smith GE, Kantarci K, *et al*. Nonamnestic mild cognitive impairment progresses to dementia with Lewy bodies. *Neurology*. 2013;81:2032-2038.

51. Kiselica AM, Johnson E, Benge JF. How impaired is too impaired? Exploring futile neuropsychological test patterns as a function of dementia severity and cognitive screening scores. *J Neuropsychol*. 2021;15:410-427.

52. Donaghy PC, McKeith IG. The clinical characteristics of dementia with Lewy bodies and a consideration of prodromal diagnosis. *Alzheimers Res Ther*. 2014;6:46.

53. Hohl U, Tiraboschi P, Hansen LA, Thal LJ, Corey-Bloom J. Diagnostic accuracy of dementia with Lewy bodies. *Arch Neurol*. 2000;57:347.

54. Tiraboschi P, Salmon DP, Hansen LA, Hofstetter RC, Thal LJ, Corey-Bloom J. What best differentiates Lewy body from Alzheimer's disease in early-stage dementia? *Brain J Neurol*. 2006;129(Pt 3):729-735.

55. Suárez-González A, Crutch SJ, Franco-Macías E, Gil-Néciga E. Neuropsychiatric symptoms in posterior cortical atrophy and Alzheimer disease. *J Geriatr Psychiatry Neurol*. 2016;29:65-71.

56. Gu Y, Kociolek A, Fernandez KK, *et al*. Clinical trajectories at the End of life in autopsy-confirmed dementia patients with Alzheimer disease and Lewy bodies pathologies. *Neurology*. 2022;98:e2140-e2149.

57. Hamilton CA, Matthews FE, Donaghy PC, *et al*. Progression to dementia in mild cognitive impairment with Lewy bodies or Alzheimer disease. *Neurology*. 2021;96:e2685–e2693.

58. McKeith IG, Ferman TJ, Thomas AJ, *et al*. Research criteria for the diagnosis of prodromal dementia with Lewy bodies. *Neurology*. 2020;94:743-755.

59. Grothe MJ, Moscoso A, Silva-Rodríguez J, *et al*. Differential diagnosis of amnestic dementia patients based on an FDG-PET signature of autopsy-confirmed LATE-NC. *Alzheimers Dement* 2022;19:1234-1244.

60. Cerami C, Della Rosa PA, Magnani G, *et al*. Brain metabolic maps in mild cognitive impairment predict heterogeneity of progression to dementia. *Neuroimage Clin*. 2015;7:187-194.

61. Swann P, O'Brien JT. Management of visual hallucinations in dementia and Parkinson's disease. *Int Psychogeriatr*. 2019;31:815-836.

62. Devi G, Scheltens P. Heterogeneity of Alzheimer's disease: Consequence for drug trials? *Alzheimers Res Ther*. 2018;10:122.

63. Stephane M. Standardized assessment of hallucinations. In: Jardri R, Cachia A, Thomas P, Pins D, eds. *The neuroscience of hallucinations*. Springer; 2013:85-104.